

Fermiology of cuprates from first principles: From small pockets to the Luttinger Fermi surface

L. Hozoi, M. S. Laad, and P. Fulde

Max-Planck-Institut für Physik komplexer Systeme, Nöthnitzer Str. 38, 01187 Dresden, Germany

(Received 19 June 2008; revised manuscript received 31 July 2008; published 10 October 2008)

Fermiology, the shape and size of the Fermi surface, underpins the low-temperature physical properties of a metal. Recent investigations of the Fermi surface of high- T_c superconductors, however, show a most unusual behavior: upon addition of carriers, “Fermi” pockets appear around nodal (hole doping) and antinodal (electron doping) regions of the Brillouin zone in the “pseudogap” state. With progressive doping, δ , these evolve into well-defined Fermi surfaces around optimal doping (δ_{opt}), with no pseudogap. Correspondingly, various physical responses, including d -wave superconductivity, evolve from highly anomalous up to δ_{opt} to more conventional beyond. Describing this evolution holds the key to understanding high-temperature superconductivity. Here, we present *ab initio* quantum chemical results for cuprates, in an attempt to provide a quantitative description of the evolution of the Fermi surface with δ . Our results constitute an *ab initio* justification for several hitherto proposed semiphenomenological theories, offering a unified basis for understanding of various unusual physical responses of cuprates.

DOI: [10.1103/PhysRevB.78.165107](https://doi.org/10.1103/PhysRevB.78.165107)

PACS number(s): 71.15.Qe, 71.27.+a, 71.28.+d, 74.72.-h

I. INTRODUCTION

Understanding high-temperature superconductivity in quasi-two-dimensional (2D), doped copper oxides remains one of the most challenging problems in condensed matter physics. In spite of varying structural and chemical details, the phase diagram of the high- T_c superconductors (HTS's) is seemingly remarkably universal: the undoped compounds with nominally one hole per Cu site are Mott insulators (MI's) due to strong electron-electron interactions.¹ Upon addition of charge carriers (doping), the cuprates turn into d -wave superconductors (d -SC) at low temperatures, $T < T_c$.¹

The “normal” state for $T > T_c$ is actually very abnormal, and radically undermines the conventional Landau theory of Fermi liquids (FL's). In the so-called underdoped (UD) regime, $\delta \ll 1$, a d -wave pseudogap (d -PG) characterizes the normal state.¹ Whether this d -PG state is the precursor of d -SC at lower T or its competitor is hotly debated.^{2,3} Around optimal doping, δ_{opt} , a “strange metal” phase with most unusual singular responses⁴ is clearly revealed: this is the celebrated non-FL metallic state that has been investigated for 20 years.¹ In the overdoped (OD) regime, $\delta > \delta_{\text{opt}}$, low- T FL behavior seems to be smoothly recovered.

Very recently, notable improvements in sample quality as well as measuring technology have finally allowed accurate mapping of the actual dispersion of the quasiparticles (QP's) and the Fermi surface (FS) of HTS's. Specifically, angle-resolved photoemission spectroscopy (ARPES) (Refs. 5–7) and Shubnikov–de Haas (SdH) quantum oscillation techniques^{8,9} reveal crucial, hitherto unmapped features of the evolution of the (*renormalized*) QP dispersion as a function of doping. Thus, these works open up the possibility, for the first time, of unearthing the link between the electronic structure and physical responses of cuprates in microscopic detail as a function of δ . Both ARPES and SdH measurements reveal a full FS consistent with conventional band-structure calculations for $\delta > \delta_{\text{opt}}$.^{5,10} However, in the UD regime, the small “Fermi” pockets inferred by SdH experiments are in deep conflict with Luttinger's theorem. For

hole-doped samples with $\delta=0.1$, the SdH results yield a carrier concentration $x_{\text{SdH}}=0.15$.⁸ Under the same conditions, the low- T Hall constant is electronlike.¹¹ How can this come about? Existing theoretical calculations cannot resolve this issue satisfactorily, and yet this finding points toward a glaring discrepancy in our understanding of the electronic structure of cuprates. Given these findings, a consistent theoretical scenario aiming to describe the unique physics of HTS's is now *constrained* to base itself upon the appropriate collective excitations stemming from the observed detailed shape and size of the FS.

Here, we address the issues raised above. Using an *ab initio* wave-function-based formalism, we describe the lowest QP bands and FS evolution with δ , with quantitative accuracy vis-à-vis recent ARPES and SdH measurements. We extend our previous work on hole-doped cuprates¹² by studying the correlated electronic structure of the “electron-doped” cuprate SrCuO₂. In the case of the p -type superconductors, we discuss the *generalized* Zhang-Rice¹³ nature of the lowest electron-removal state. Further, motivated by the SdH and Hall-effect experiments mentioned above, we point out possible implications of our results in light of these experiments, as well as their connection to earlier model-based and semiphenomenological theories, in detail. Our calculations confirm the view¹⁴ that the unique properties of cuprates are those of a 2D doped MI.

II. THEORETICAL FRAMEWORK

The correlation-induced renormalization effects on the valence and conduction energy bands are remarkably strong in cuprates. Early attempts to describe these effects were based on the t - J model¹ and indicated the crucial role played by the strong antiferromagnetic (AF) couplings in reducing itinerance. In the three-band context, it was suggested that a doped oxygen hole would induce short-range ferromagnetic (FM) correlations among adjacent Cu sites.¹⁵ If the extra hole delocalizes over all four equivalent ligands of a given CuO₄ plaquette,¹³ these FM correlations would involve Cu

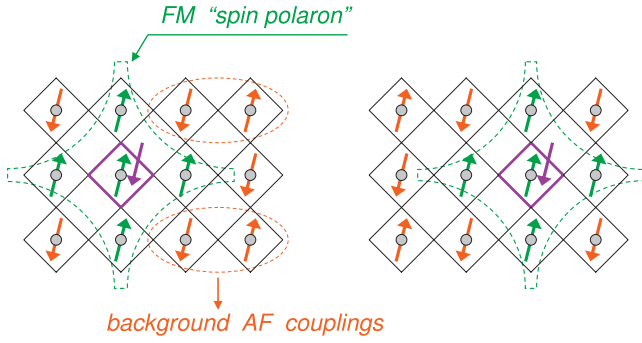


FIG. 1. (Color) Ferromagnetic correlations (green) among Cu sites around a doped oxygen hole (violet) as inferred from CASSCF calculations. Farther spin couplings are antiferromagnetic (red). The motion of the oxygen hole is coherent when the FM spin polarization “cloud” at adjacent Cu sites moves solidarily with the hole. The O ligands are at the vertices of the square plaquettes; the Cu ions are shown as gray dots.

sites on five plaquettes,¹⁶ as shown in Fig. 1. Since the mobility of this entity is expected to be small, it is often referred to as a FM “spin polaron.”

An accurate investigation of the structure of such composite objects calls for methods that allow an unbiased treatment of the various (competing) interactions in the CuO_2 plane. A fundamental point underlying the physics of cuprates is the interplay between electron localization effects as a result of strong repulsive interactions and itinerant behavior as a result of translational symmetry and intersite orbital overlap. Standard band theories based upon the density-functional model [and the local-density approximation (LDA)] mainly emphasize the latter aspect. Though LDA provides rather good results for weakly correlated solids, its limited ability to describe correlated d (and f) electrons is well documented. With the advent of dynamical mean-field theory (DMFT), this basic conflict has been partially resolved.¹⁷ In particular, much progress in describing the FS’s of real materials, along with their one-particle spectral functions, has been possible. However, this is still some distance from being a totally *ab initio* approach, since the actual correlations are approximated by local (Hubbard) *parameters*. Use of constrained LDA to estimate these parameters entails an uncertainty on the order of 20%, while their self-consistent estimation within LDA/LDA+DMFT is fraught with insurmountable problems.¹⁸

An alternative approach bases itself on state-of-the-art quantum chemical (QC) methods.¹⁹ In molecular systems, wave-function-based quantum chemistry provides a rigorous theoretical framework for addressing the electron correlation problem.²⁰ A real-space, QC-based treatment is then a natural starting point in dealing with Mott physics in d -metal solid-state compounds. As shown below, the \mathbf{k} -dependent energy bands can be recovered at a later stage after accounting for the ubiquitous strong short-range correlation effects.

The strategy is to use a sufficiently large cluster, \mathcal{C} , cut out from the infinite solid and properly embedded in some effective lattice potential, capable of describing these crucial short-range correlations accurately. The presence of partially filled d -electron shells requires a multiconfiguration repre-

sentation of the many-electron wave function. The complete-active-space (CAS) self-consistent-field (SCF), CASSCF, method²¹ provides precisely such a framework (see Sec. II A for details). It can, for example, describe spin correlation effects such as the Anderson superexchange in MI’s (Ref. 22) and the double-exchange in mixed-valence systems.²³ For undoped cuprates, with formally one $3d_{x^2-y^2}$ electron per Cu site, the CAS wave function is similar to the variational wave function used in numerical studies of the 2D, one-band Hubbard model.²⁴ The main difference is that *all* integrals, including intersite Coulomb and exchange terms, are computed here in a totally *ab initio* way. In particular, the lower, completely filled levels, e.g., the O $2s$ and $2p$ orbitals, do affect (i.e., screen) the actual interactions among the active electrons by readjusting themselves to fluctuations within the active orbital space.

The dispersion of d -like states on a square lattice is given by the following relation:

$$\epsilon(\mathbf{k}) = -2t(\cos k_x a + \cos k_y a) + 4t' \cos k_x a \cos k_y a - 2t''(\cos 2k_x a + \cos 2k_y a),$$

where t , t' , t'' are the hopping integrals between nearest-neighbor (NN), second-NN, and third-NN sites and the effective site is one CuO_4 plaquette.¹³ LDA calculations yield t values of 0.4–0.5 eV and a ratio between the NN and second-NN hoppings $t'/t \approx 0.17$ for La_2CuO_4 and 0.33 for $\text{Tl}_2\text{Ba}_2\text{CuO}_6$.^{25,26} In contrast, the CASSCF calculations predict a *renormalized* NN hopping $t=0.135$ eV in La_2CuO_4 .^{12,16} Here, we describe how the detailed QP dispersion can be obtained with quantitative accuracy, for *both* hole and electron-addition states. The effective hoppings are computed by using the overlap, S_{ij} , and Hamiltonian, H_{ij} , matrix elements between $(N \mp 1)$ -particle wave functions having the additional particle (hole or electron) located on different plaquettes (i, j, \dots) of a given cluster. Each of these $(N \mp 1)$ wave functions, $|\Psi_i^{N \mp 1}\rangle$, is obtained by *separate* CASSCF optimizations. A similar scheme was previously applied to simpler, noncontroversial systems such as diamond, silicon, and MgO.^{27–29} It accounts for both charge^{27,28} and spin^{12,16} polarization and relaxation effects in the nearby surroundings; see Fig. 1. For degenerate (i.e., $H_{ii}=H_{jj}$) $(N \mp 1)$ states, $t \equiv (\epsilon_j - \epsilon_i)/2 = (H_{ij} - S_{ij}H_{ii})/(1 - S_{ij}^2)$, where ϵ_i and ϵ_j are the eigenvalues of the 2×2 secular problem. For nondegenerate ($H_{ii} \neq H_{jj}$) states, $t \equiv 1/2[(\epsilon_j - \epsilon_i)^2 - (H_{jj} - H_{ii})^2/(1 - S_{ij}^2)]^{1/2}$. The S_{ij} and H_{ij} terms are computed using the state-interaction (SI) method.³⁰ Correlation effects beyond CASSCF on the on-site matrix elements H_{ii} are calculated by multiconfigurational second-order perturbation theory, CASPT2.³¹ The short-range magnetic correlations are included in our clusters by adding extra CuO_4 units around those plaquettes directly involved in the hopping process; see Fig. 2.

The basic assumption we are making in our study is the quasiparticle approximation, see, e.g., Ref. 19. Everything going beyond that approximation would require a Green’s function formulation. The incoherent processes leading, e.g., to satellite structures are beyond the scope of our present calculations. Quasiparticle interactions are not accounted for

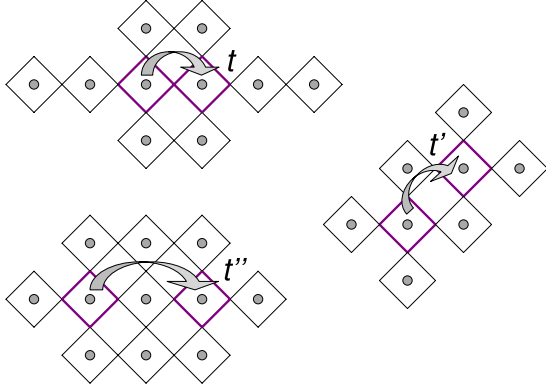


FIG. 2. (Color online) Sketch of the finite clusters employed for the calculation of the effective valence-band and conduction-band hoppings.

either. Nevertheless, the strong correlation effects on the band structure are treated accurately and the calculated quasiparticle dispersion is that of a doped Hubbard system.

A. Computational details

In the CASSCF approach,^{20,21} the wave function is written as a linear combination of configuration state functions (CSF's) $|m\rangle$, $|\Psi\rangle = \sum_m C_m |m\rangle$. These CSF's are spin- (and symmetry-) adapted combinations of Slater determinants (SD's), i.e., eigenfunctions of the operators for the projected and total spins. In turn, the SD's are constructed from a set of real and orthonormal spin orbitals $\{\phi_p(\mathbf{r}, \sigma)\}$, where \mathbf{r} and σ are the spatial and spin coordinates, respectively. In this work, an initial guess for these orbitals is obtained from a Hartree-Fock calculation for a hypothetical Cu $3d^{10}$, O $2p^6$ closed-shell configuration of the Cu and O species.

In determining the CASSCF wave function, the orbitals are variationally optimized simultaneously with the coefficients of the CSF's. The orbitals employed for expressing the wave function are thus the optimal orbitals for the state at hand and do not introduce a bias toward a particular configuration. Three different sets of orbitals are used in CASSCF: (i) the inactive levels, doubly occupied in all configurations, (ii) the virtual orbitals, unoccupied in all configurations, and (iii) the active orbital set, where no occupancy restrictions are imposed. For undoped cuprates, with formal Cu $3d^9$ and O $2p^6$ valence states, the minimal active space would include the partially occupied in-plane Cu $3d_{x^2-y^2}$ orbitals. If extra holes are created, the active space must be enlarged with orbitals from the inactive group. Each additional doped hole requires one orbital to be transferred from the inactive to the active space. For the lowest electron-removal state, for example, the orbital added to the active space turns into a Zhang-Rice (ZR) type $p-d$ composite¹³ in the variational calculation, localized on a given CuO₄ plaquette. With regard to the electron-addition conduction-band states, these turn out to have Cu $3d^{10}$ character and, in a first approximation, an active orbital space including only the $3d_{x^2-y^2}$ levels would suffice.

So-called dynamic correlation effects²⁰ for the on-site matrix elements H_{ii} were computed using second-order pertur-

TABLE I. Hopping ME's for ZR-type states in La₂CuO₄ and electron-addition Cu d^{10} states in SrCuO₂. The bare hoppings were computed by imposing high-spin couplings among the nearby Cu sites.

Hopping ME's (eV)	Bare	Renormalized
"ZR" state		
t	0.540	0.135
t'	0.305	0.010
t''	0.115	0.075
d^{10} state		
t	0.290	0.115
t'	0.130	0.130
t''	0.045	0.015

bation theory (the CASPT2 method³¹). The Cu $3d$ and O $2s$, $2p$ electrons on five plaquettes (i.e., the ZR plaquette and the two apical ligands for that plaquette plus the four NN plaquettes) were correlated. All calculations were performed with the quantum chemical software MOLCAS.³² For the ions of the plaquettes directly involved in the hopping process, all-electron basis sets (BS's) of triple-zeta quality were applied. These were Gaussian-type atomic-natural-orbital BS's from the MOLCAS library,³² with the following contractions:²⁰ Cu(21s15p10d)/[5s4p3d] and O(14s9p)/[4s3p]. The core electrons of the remaining ions of each cluster, see Fig. 2, were represented by effective core potentials (ECP's), i.e., Cu ECP's plus valence double-zeta BS's (Ref. 33) and O ECP's with triple-zeta BS's.³⁴ To describe the finite charge distribution at the sites in the immediate neighborhood of the cluster, we model those ions by effective ion potentials.³⁵ Beyond these neighbors, we use large arrays of point charges (PC's) that reproduce the crystal Madelung field within the cluster region. Apical ligands are explicitly included in our calculations only for the "active" plaquettes. Other apex oxygens are represented by formal PC's. That the charge populations of the Cu $3d$ and active O $2p$ orbitals are not sensitive to the size and shape of the clusters we use was shown in Ref. 16. We employed the crystal structure measured by Cava *et al.*³⁶ for La₂CuO₄ and by Smith *et al.*³⁷ for SrCuO₂.

III. QUASIPARTICLE BANDS AND ARPES

In earlier work,^{12,16} the p -type HTS La₂CuO₄ was investigated. Here, we extend that work to study the n -type HTS SrCuO₂. For the sake of completeness, we present the detailed description of *both* hole- and electron-doped cuprates in this paper. Renormalized hopping matrix elements (ME's) for ZR-type states in La₂CuO₄ and electron-addition states in SrCuO₂, involving neighbors up to the third order, are listed in Table I. For comparison, "unrenormalized" (or bare) hoppings were also computed, by imposing a FM arrangement of spins at the nearby Cu sites, i.e., a FM lattice. The bare hoppings are substantially smaller for the $(N+1)$ Cu d^{10} states because the Cu $3d$ functions are more compact as compared to the O $2p$ orbitals.

Interestingly, for the electron-addition states, each of the effective hoppings changes by less than 15% from La_2CuO_4 to SrCuO_2 (not shown in Table I), although the crystalline structures of the two compounds are quite different, with no apical oxygens for the latter. On the other hand, no ZR-type solution was obtained for the electron-removal states in SrCuO_2 , which qualitatively confirms the experimental findings: for in-plane lattice constants $a \geq 3.87 \text{ \AA}$ ($a = 3.925 \text{ \AA}$ in SrCuO_2), the CuO_2 planes do not readily accept holes in the O bands.³⁷ We also found that the energy difference between the electron-addition [$E(N+1)$] and electron-removal [$E(N-1)$] states relative to the N -electron state, given by $\Delta E = E(N+1) + E(N-1) - 2E(N)$, is about 5 eV.³⁸ Thus, the ground state of the undoped N -electron system is found to be a Mott-Hubbard-type insulating state, in agreement with standard knowledge for the parent cuprate compounds.

In effective one-band models,^{1,13} the ZR p - d state is regarded as a vacant, or unoccupied, d -like site. Consequently, there is no renormalization of the second-NN and third-NN hoppings t' and t'' because these connect sites of the same magnetic sublattice. In contrast, the interplay between short-range FM correlations and longer-range AF couplings (see the sketch in Fig. 1) produces large renormalization effects for *all* hopping ME's in our approach. For t' and t'' , in particular, the hopping of the $2p$ hole implies coupled, Cu and O spin “flips” on the two plaquettes directly involved in the hopping process. Nevertheless, spin correlations decay rapidly with distance and so the renormalization effects are less drastic for the third-NN ME, t'' . We thus find $t'' \approx t/2$ and $t' \ll t$, a rather remarkable result.

For the description of the electron-addition d^{10} states, an effective one-band model¹ is seen to be justified. As shown in Table I, in this case only t is substantially affected by nonlocal spin correlations. Hence, for the $(N+1)$ states, the renormalized hoppings satisfy $t' \approx t$, an equally remarkable result. The particle-hole asymmetry, see Fig. 3, is now readily understood from the very different t'/t and t''/t values for the $(N-1)$ (ZR-type) and $(N+1)$ (Cu d^{10}) bands.

Doping of the CuO_2 planes is achieved by chemical substitution in the “reservoir” layers. The dopant carriers must quantum mechanically tunnel from the reservoir to the planes: this necessarily involves the apical O $2p_z$, Cu $3d_{z^2}$ and Cu $4s$ orbitals, causing additional renormalization of the planar QP's from these apical charge-transfer interactions. Hence, we extended our calculations to include configurations where an electron is removed from or added to the Cu $3d_{z^2}$ or Cu $4s$ orbital.

Only the Cu $3d_{z^2}$ ($N-1$) state gave rise to considerable renormalization of the planar QP dispersion. While the on-site mixing between the ZR and d_{z^2} ($N-1$) configurations and the NN hopping between degenerate d_{z^2} hole states are negligible, the *intersite* off-diagonal hopping is large. With sets of orbitals individually optimized for each $(N-1)$ state, this off-diagonal ME is $t_m = 0.20$ eV, larger than the value reported in Ref. 12, where the lowest d_{z^2} hole state was expressed in terms of orbitals optimized over an average of several excited states involving different couplings among the nearby Cu spins. In \mathbf{k} space, the hybridization ME between the ZR-type and d_{z^2} bands reads $\gamma_m(\mathbf{k}) = t_m(\cos k_x a - \cos k_y a)$. Further, on-site, the ZR-type and d_{z^2} ($N-1$) states

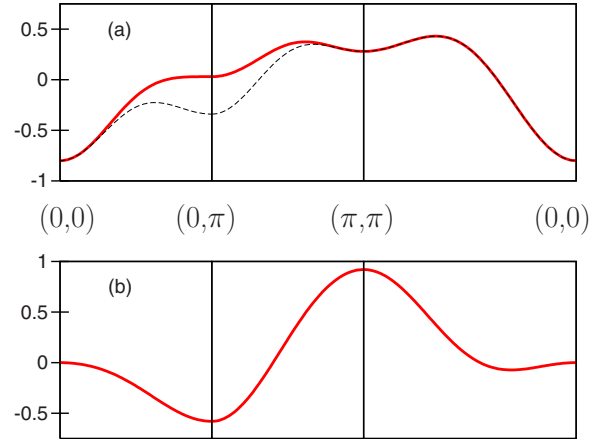


FIG. 3. (Color online) (a) The ZR-type electron-removal band for La_2CuO_4 in the 2D Brillouin zone, without including the interaction with the $d_{3z^2-r^2}$ hole state (dashed line) and after including this interaction (thick red line). For clarity, the $d_{3z^2-r^2}$ band is not shown in the figure. The zero of energy is the value of the on-site Hamiltonian ME of the ZR-type state, H_{ii}^{ZR} . (b) QP dispersion for the electron-addition Cu d^{10} state in SrCuO_2 . The reference energy is the value of the on-site Hamiltonian ME, $H_{ii}^{d^{10}}$. Units of eV are used in both panels.

are separated by an energy $\Delta\epsilon$. It turns out that the correlation-induced corrections to the CASSCF energy separation are substantial, changing this quantity from 0.60 eV (Ref. 12) to $\Delta\epsilon = 1.70$ at the CASPT2 level. Such corrections are usually small, for both the on-site *relative* energies²² and hoppings.^{16,28} Nevertheless, corrections as large as 0.9 eV have been found before for the relative energy of the $^1A_{1g}$ state of the d^8 manifold in NiO,²² for example.²⁹

The quantum chemical calculations allow an analysis of the strength of correlation effects in doped cuprates. The dominant contribution to the lowest electron-removal state is a superposition of three configurations, $|d_{x^2-y^2}^1 p_\sigma^1\rangle$, $|d_{x^2-y^2}^2 p_\sigma^0\rangle$, and $|d_{x^2-y^2}^0 p_\sigma^2\rangle$ (hole notation), where p_σ denotes the in-plane ZR-type combination of O $2p_{x,y}$ orbitals on one CuO_4 plaquette. The weights of these configurations in the CASSCF wave function are 0.70, 0.14, and 0.11, respectively.³⁹ In the Heitler-London limit, i.e., for $U \rightarrow \infty$, the weight of the $|d_{x^2-y^2}^2 p_\sigma^0\rangle$ configuration would vanish since double hole occupation of a Cu site is excluded in that limit. Our *ab initio* data indicate thus that the quantum chemical picture deviates somewhat from the original Heitler-London-type model of Zhang and Rice.¹³ Moreover, there are contributions of a few percent to the multiconfigurational wave function which are related to interplaquette d - p - d excitations and responsible for the FM d - d correlations around the O $2p$ hole. Additionally, our incorporation of the d_{z^2} hole state and its mixing with the (x^2-y^2) hole state goes beyond the models hitherto considered, where, to the best of our knowledge, such effects have not been discussed within a correlated framework. The detailed consequences of these findings in the context of a “minimal” model for cuprates will be treated at length in future work. In what follows, we discuss how the above findings facilitate a detailed theory-experiment comparison.

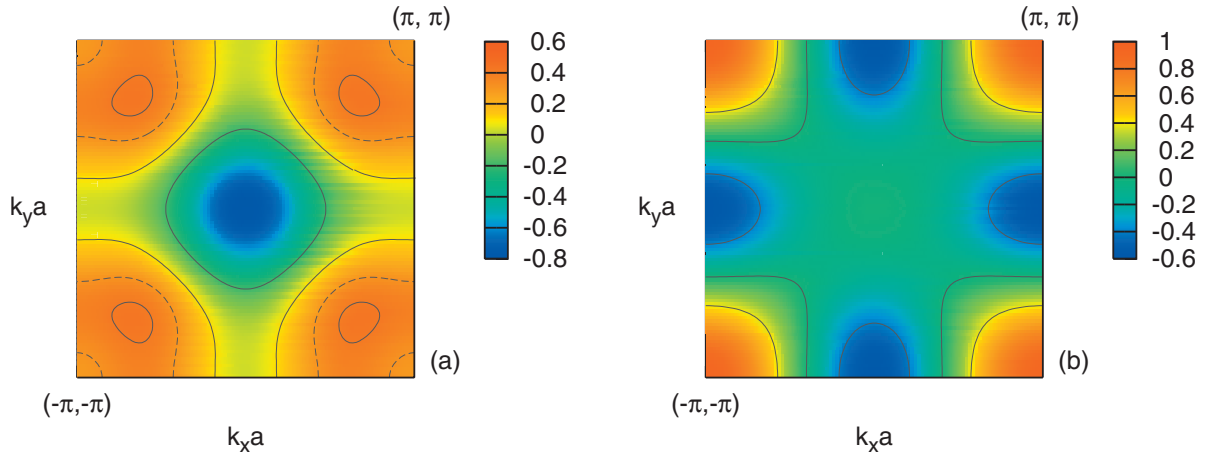


FIG. 4. (Color) (a) 2D color map for the ZR-type QP dispersion in La_2CuO_4 , including the effect of the ZR- d_{z^2} hole interaction. In a rigid-band picture, the constant-energy (CE) contours (black curves) illustrate the evolution of the FS with *hole doping*, from small (hole) pockets in the nodal region for deeply UD samples to a large holelike FS at intermediate dopings and an electronlike shape in the OD regime (Ref. 5). For a narrow doping interval in the UD regime, the “FS” is defined by eight contours (see the dashed curves), with *both* holelike sheets and electron pockets centered at the corners of the Brillouin zone. The latter are related to the small dip in the dispersion at the (π, π) point, see Fig. 3(a), and have been also inferred from Hall-effect measurements (Ref. 11) (b) Color map for the electron-addition $\text{Cu } d^{10}$ states in SrCuO_2 . The CE contours reproduce the experimentally observed evolution of the FS with *electron doping*, from small electron pockets in the antinodal region for the lightly doped regime to a large holelike FS at high doping (Refs. 5 and 48). The same energy scales as in Fig. 3 are used.

It is now straightforward to diagonalize the \mathbf{k} -dependent 2×2 matrix,

$$\begin{pmatrix} \epsilon_{\text{ZR}}(\mathbf{k}) & \gamma_m(\mathbf{k}) \\ \gamma_m(\mathbf{k}) & \epsilon_{z^2}(\mathbf{k}) + \Delta\epsilon \end{pmatrix},$$

to yield the renormalized bands. This constitutes a nontrivial extension of the three-band Hubbard model, where the additional renormalization from the apical link is not considered. Shown in Fig. 3(a) is the resulting dispersion of a ZR-type singlet generated by a doped hole. We call that object a quasiparticle. The figure tells us what the energy of the quasiparticle is once its momentum \mathbf{k} is given. The dispersion of the ZR-type band shows good agreement with the dispersion of the lowest ARPES band reported for La_2CuO_4 by Ino *et al.*⁴⁰ In particular, the flat dispersion around $(\pm\pi, 0)$ and $(0, \pm\pi)$, the maximum near $(\pm\pi/2, \pm\pi/2)$, and a renormalized bandwidth of nearly 1 eV are all reproduced in the theoretical results. The importance of the ZR- z^2 mixing is apparent: it is *required* to generate pronounced flattening of the bands in the antinodal regions of the Brillouin zone. Given their controversial interpretation,⁴¹ we did not attempt to describe the “waterfalls” seen in ARPES. Theoretically, the study of such structures requires an analysis of the *incoherent* part of the spectral function.^{17,42,43} For the $\text{Cu } d^{10}$ states, see Fig. 3(b), a lack of detailed data for ARPES line shapes in n -type cuprates precludes a direct comparison between theory and experiment.

Knowledge of the QP dispersion enables us to study the evolution of the *renormalized* FS as a function of doping. Thereby the following features have to be kept in mind. Since the QP is a ZR-type singlet state we cannot have more than one singlet per plaquette. Provided the character of the QP’s would remain unchanged with increasing hole doping,

we would be able to fill the band with one doped hole per plaquette, i.e., per \mathbf{k} state. However, that is not what is happening, as is well known from studies of the Hubbard model, when an originally full lower Hubbard band is depleted by hole doping. Here, like in the Hubbard model, the QP band can accommodate an increasing number of holes as the hole concentration increases. Eventually one may fill each \mathbf{k} state with two instead of one hole, and the well-known Luttinger theorem for the FS does apply. The reason is that with increasing hole doping correlations become less and less important. Certainly, for heavy overdoping, our present calculations are quantitatively not reliable.

Assuming that the chemical potential shifts downward (upward) with hole (electron) doping, an assumption supported by independent experiments,^{44,45} we plot the evolution of the FS for *both* hole and electron-doped cuprates in Fig. 4. We simulate doping effects by a progressive downward shift (hole doping) and upward shift (electron doping) of the Fermi energy, E_F . We find that small hole pockets in the nodal region comprise the “FS” in the deeply UD regime.^{8,9} These pockets are centered in the region(s) between the $(\pm\pi/2, \pm\pi/2)$ and $(\pm\pi, \pm\pi)$ points, as also predicted by projection-technique^{42,43} and cellular DMFT (Ref. 46) calculations for the Hubbard system. Recent ARPES data for $\text{La}_{2-x}\text{Sr}_x\text{CuO}_4$ samples with $x=0.03$ show indeed that spectral weight is mainly found between the $(\pm\pi/2, \pm\pi/2)$ and $(\pm\pi, \pm\pi)$ points.⁴⁷ Whether the disconnected features observed in photoemission^{5,47} correspond to the inner arc profiles of the holelike pockets predicted theoretically is an unsettled issue. The electron-removal spectral weight in the region between the $(\pm\pi/2, \pm\pi/2)$ and $(\pm\pi, \pm\pi)$ points is expected to be vanishingly small because of the strong drop in the quasiparticle coherence beyond the AF zone boundary. We believe that the “discrep-

ancy” between the quantum oscillation data^{8,9} (which show closed pockets) and the ARPES spectra⁵ (which show the Fermi “arcs”) in the underdoped regime is related to the fact that the first give information on the QP dispersion, while the second map both the dispersion *and* the \mathbf{k} -dependent damping of QP’s.

For slightly higher δ , smaller, electronlike pockets centered around *the corners* of the Brillouin zone are also clearly resolved; see Fig. 4(a). With further doping, these progressively evolve into a large holelike FS,⁵ implying a FS reconstruction close to δ_{opt} . At a critical value $\delta = \delta_c$, the FS changes from holelike ($\delta < \delta_c$) to electronlike ($\delta > \delta_c$), in accord with results from ARPES.⁵

Similar agreement of the FS vis-à-vis experiment⁴⁸ is also obtained for the n -type cuprates: small pockets centered around the $(\pm\pi, 0)$ and $(0, \pm\pi)$ points evolve into a holelike FS with progressive electron doping. Our *ab initio* results capture such effects: hitherto, these have been (partially) described within *effective*, one-^{42,46,49} or three-band⁵⁰⁻⁵² models with parametrized couplings.

IV. BROADER IMPLICATIONS

Our results constitute an *ab initio* derivation of the “hot-spot-cold-spot” phenomenology,⁵³ also seen in cluster-DMFT work on the 2D Hubbard model.¹⁷ There, the QP scattering rate is strongly \mathbf{k} dependent as the FS is traversed. This is manifest in our computed FS: the pronounced dispersion of the nodal QP’s implies weaker QP scattering around \mathbf{k}_n , in marked contrast to the antinodal region, where strong band flattening is indicative of strong QP scattering and very short QP lifetimes. Further, the renormalized t, t', t'' imply *intrinsically* frustrated hopping: interestingly, the importance of frustrated kinetic energy to the high- T_c problem has been discussed at length in the resonating valence bond (RVB) model of Anderson.¹⁴ We show that *both* these seemingly disparate features arise from the same underlying microscopic mechanism: strongly anisotropic renormalization of carrier motion by strong, short-range spin correlations.

Interestingly, in Hubbard-type models, large t' (or t'') open the door to additional exotic phases, like d -wave nematic,⁵⁴ d -density wave,⁵⁵ and valence-bond⁵⁶ ordered phases. These have been invoked as possible competitors of d -SC in various semiphenomenological contexts. Our work establishes the intimate connection between these putative instabilities and short-range spin correlations characteristic of a (lightly doped) MI.

Our findings have remarkable implications for the interpretation of a host of experiments probing the unusual “normal”-state physical responses of the cuprates as a function of doping. First, the UD p -type cuprates are revealed to be nodal metals for small δ , as inferred by ARPES.^{6,7} All the “nodal metal” phenomenology¹ can now be provided an *ab initio* justification in light of our results. Coherent nodal QP’s also naturally explain the “good metal” thermal conductivity in the UD region.⁵⁷ Additionally, the SdH quantum oscillation frequencies Ω now correspond to coherent carrier orbits in the “pockets.”^{8,9} Under the assumption that a \mathbf{k} state cannot contain more than one QP, the Onsager-Lifshitz formula

reads $\Omega = \Phi_0 A / (2\pi)^2$, with $\Phi_0 = hc/e$ as the flux quantum and $A = (2\pi)^2 x / 4a^2$ as the area of the pocket for x carriers in \mathbf{k} space. It tells us that $\Omega(x) \sim x$. Our finding of additional electronlike pockets around (π, π) in the hole-doped case offers a route toward a resolution of one of the central controversies surrounding recent SdH experiments, where $x_{\text{SdH}} = 0.15$ for the $\delta = 0.10$ cuprates.⁸ While this is irreconcilable with theories having only hole pockets, our finding of additional electronlike sheets can reconcile the SdH results with the \mathbf{k} state counting for $\delta \approx 0.1$.^{8,9} Moreover, the Hall constant $R_H(x)$ is now expected to track the evolution of the renormalized FS with doping. Depending upon the concentrations of hole and electron carriers n_h and n_e , with $n_h > n_e$, and the mobilities μ_h and μ_e , R_H may change sign from holelike to electronlike with T ,¹¹ reconciling the SdH (Refs. 8 and 9) and Hall-effect¹¹ data. This is a different picture compared to the alternative of a 3/2-Fermi liquid,⁵⁸ proposed exactly in this connection, where the possibility of $R_H < 0$ is not clear.

Finally, what about superconductivity? Given the small number, δ , of nodal QP’s in the UD regime, d -SC will result from pairing of these quasicohherent fermionic entities. Without going into the nature of the pairing mechanism, the above implies that $T_c(\delta) \sim \delta$ for $\delta \ll 1$. So the superfluid density at $T=0$ will decrease *linearly* as δ is reduced, implying that upon underdoping d -SC will be progressively destroyed by order parameter phase fluctuations, which grow as the MI is approached. This implies non-BCS (large) values of $2\Delta/k_B T_c$ and strong vortex-liquid-like effects above T_c for UD cuprates. These have indeed been invoked in connection with the anomalous “giant” Nernst effect in UD superconductors.² However, once a full FS develops, d -SC would be expected to revert back to a more conventional BCS-type variety,¹ with identical scaling for the nodal and antinodal gaps.

V. CONCLUSIONS

To summarize, we have implemented a first-principles, wave-function-based calculation of correlated hole and electron-addition quasiparticle states in layered cuprates. In addition to quantitatively describing the dispersion of the ZR-type band, our work reproduces the FS evolution as a function of doping, in good agreement with a host of recent ARPES and quantum oscillation experiments. Our finding of large longer-range effective hoppings implies intrinsically frustrated carrier kinetic energy, in agreement with Anderson’s RVB ideas.¹⁴ The very different behavior of hole and electron-doped cuprates is clearly manifested as originating from very different quantum chemical and spin correlation “backgrounds.” These give rise to very different hopping parameters t, t'', t''' in the hole- or electron-doped cuprates, implying asymmetric T - x phase diagrams. Seen from this perspective of renormalization of carrier hoppings by strong, short-range spin fluctuations, the FS “reconstruction” with doping,¹¹ as well as the famed nodal-antinodal dichotomy in the UD systems, are both understood in terms of \mathbf{k} -space differentiation of QP states in the 2D doped MI. Phenomenologically, the computed evolution of the FS with δ goes

hand-in-hand with the observed evolution of d -SC from a strongly non-BCS, phase fluctuation dominated type, to a more conventional BCS type with progressive doping, benchmarking the crucial relevance of fermiology in cuprates.

ACKNOWLEDGMENTS

We thank C. de Graaf for making available to us the analysis for the composition of the generalized ZR wave function in terms of localized Cu $3d_{x^2-y^2}$ and O $2p_{x,y}$ orbitals.

- ¹P. A. Lee, N. Nagaosa, and X.-G. Wen, *Rev. Mod. Phys.* **78**, 17 (2006).
- ²Y. Wang, L. Li, and N. P. Ong, *Phys. Rev. B* **73**, 024510 (2006).
- ³C. M. Varma, *Phys. Rev. B* **73**, 155113 (2006).
- ⁴D. van der Marel, H. J. A. Molegraaf, J. Zaanen, Z. Nussinov, F. Carbone, A. Damascelli, H. Eisaki, M. Greven, P. H. Kes, and M. Li, *Nature (London)* **425**, 271 (2003).
- ⁵A. Damascelli, Z. Hussain, and Z.-X. Shen, *Rev. Mod. Phys.* **75**, 473 (2003).
- ⁶K. Tanaka, W. S. Lee, D. H. Lu, A. Fujimori, T. Fujii, Risdiana, I. Terasaki, D. J. Scalapino, T. P. Devereaux, Z. Hussain, and Z.-X. Shen, *Science* **314**, 1910 (2006).
- ⁷A. Kanigel, M. R. Norman, M. Randeria, U. Chatterjee, S. Souma, A. Kaminski, H. M. Fretwell, S. Rosenkranz, M. Shi, T. Sato, T. Takahashi, Z. Z. Li, H. Raffy, K. Kadowaki, D. Hinks, L. Ozyuzer, and J. C. Campuzano, *Nat. Phys.* **2**, 447 (2006).
- ⁸N. Doiron-Leyraud, C. Proust, D. LeBoeuf, J. Levallois, J.-B. Bonnemaison, R. Liang, D. A. Bonn, W. N. Hardy, and L. Taillefer, *Nature (London)* **447**, 565 (2007).
- ⁹E. A. Yelland, J. Singleton, C. H. Mielke, N. Harrison, F. F. Balakirev, B. Dabrowski, and J. R. Cooper, *Phys. Rev. Lett.* **100**, 047003 (2008).
- ¹⁰M. Abdel-Jawad, M. P. Kennett, L. Balicas, A. Carrington, A. P. Mackenzie, R. H. McKenzie, and N. E. Hussey, *Nat. Phys.* **2**, 821 (2006).
- ¹¹D. LeBoeuf, N. Doiron-Leyraud, J. Levallois, R. Daou, J.-B. Bonnemaison, N. E. Hussey, L. Balicas, B. J. Ramshaw, R. Liang, D. A. Bonn, W. N. Hardy, S. Adachi, C. Proust, and L. Taillefer, *Nature (London)* **450**, 533 (2007).
- ¹²L. Hozoi and M. S. Laad, *Phys. Rev. Lett.* **99**, 256404 (2007).
- ¹³F. C. Zhang and T. M. Rice, *Phys. Rev. B* **37**, 3759 (1988).
- ¹⁴P. W. Anderson, *The Theory of Superconductivity in the High- T_c Cuprates* (Princeton University Press, Princeton, NJ, 1997).
- ¹⁵V. J. Emery and G. Reiter, *Phys. Rev. B* **38**, 4547 (1988).
- ¹⁶L. Hozoi, S. Nishimoto, and C. de Graaf, *Phys. Rev. B* **75**, 174505 (2007).
- ¹⁷G. Kotliar, S. Y. Savrasov, K. Haule, V. S. Oudovenko, O. Parcollet, and C. A. Marianetti, *Rev. Mod. Phys.* **78**, 865 (2006).
- ¹⁸I. V. Solov'yev and M. Imada, *Phys. Rev. B* **71**, 045103 (2005).
- ¹⁹P. Fulde, *Adv. Phys.* **51**, 909 (2002).
- ²⁰T. Helgaker, P. Jørgensen, and J. Olsen, *Molecular Electronic-Structure Theory* (Wiley, Chichester, 2000).
- ²¹B. O. Roos, P. R. Taylor, and P. E. M. Siegbahn, *Chem. Phys.* **48**, 157 (1980).
- ²²C. de Graaf, Ph.D. thesis, University of Groningen, 1998.
- ²³A. Stoyanova, C. Sousa, C. de Graaf, and R. Broer, *Int. J. Quantum Chem.* **106**, 2444 (2006).
- ²⁴M. Capello, F. Becca, M. Fabrizio, S. Sorella, and E. Tosatti, *Phys. Rev. Lett.* **94**, 026406 (2005).
- ²⁵E. Pavarini, I. Dasgupta, T. Saha-Dasgupta, O. Jepsen, and O. K. Andersen, *Phys. Rev. Lett.* **87**, 047003 (2001).
- ²⁶P. R. C. Kent, T. Saha-Dasgupta, O. Jepsen, O. K. Andersen, A. Macridin, T. A. Maier, M. Jarrel, and T. C. Schulthess, *Phys. Rev. B* **78**, 035132 (2008).
- ²⁷U. Birkenheuer, P. Fulde, and H. Stoll, *Theor. Chem. Acc.* **116**, 398 (2006).
- ²⁸L. Hozoi, U. Birkenheuer, P. Fulde, A. Mitrushchenkov, and H. Stoll, *Phys. Rev. B* **76**, 085109 (2007).
- ²⁹See also L. Hozoi, U. Birkenheuer, H. Stoll, and P. Fulde, arXiv:0804.2626 (unpublished).
- ³⁰P.-Å. Malmqvist, *Int. J. Quantum Chem.* **30**, 479 (1986).
- ³¹K. Andersson, P.-Å. Malmqvist, B. O. Roos, A. J. Sadlej, and K. Wolinski, *J. Phys. Chem.* **94**, 5483 (1990).
- ³²MOLCAS 6, Department of Theoretical Chemistry, University of Lund, Sweden.
- ³³L. Seijo, Z. Barandíaran, and S. Huzinaga, *J. Chem. Phys.* **91**, 7011 (1989).
- ³⁴A. Bergner, M. Dolg, W. Küchle, H. Stoll, and H. Preuss, *Mol. Phys.* **80**, 1431 (1993).
- ³⁵F. Illas, J. Rubio, and J. C. Barthelat, *Chem. Phys. Lett.* **119**, 397 (1985); W. R. Wadt and P. J. Hay, *J. Chem. Phys.* **82**, 284 (1985).
- ³⁶R. J. Cava, A. Santoro, D. W. Johnson, and W. W. Rhodes, *Phys. Rev. B* **35**, 6716 (1987).
- ³⁷M. G. Smith, A. Manthiram, J. Zhou, J. B. Goodenough, and J. T. Markert, *Nature (London)* **351**, 549 (1991).
- ³⁸This is an overestimate since long-range polarization effects are not accounted for; see for example the discussion in Refs. 19 and 27–29.
- ³⁹C. de Graaf (private communication).
- ⁴⁰A. Ino, C. Kim, M. Nakamura, T. Yoshida, T. Mizokawa, Z.-X. Shen, A. Fujimori, T. Kakeshita, H. Eisaki, and S. Uchida, *Phys. Rev. B* **62**, 4137 (2000).
- ⁴¹D. S. Inosov, J. Fink, A. A. Kordyuk, S. V. Borisenko, V. B. Zabolotnyy, R. Schuster, M. Knupfer, B. Büchner, R. Follath, H. A. Dürr, W. Eberhardt, V. Hinkov, B. Keimer, and H. Berger, *Phys. Rev. Lett.* **99**, 237002 (2007).
- ⁴²Y. Kakehashi and P. Fulde, *Phys. Rev. Lett.* **94**, 156401 (2005).
- ⁴³Y. Kakehashi and P. Fulde, *J. Phys. Soc. Jpn.* **76**, 074702 (2007).
- ⁴⁴F. Ronning, T. Sasagawa, Y. Kohsaka, K. M. Shen, A. Damascelli, C. Kim, T. Yoshida, N. P. Armitage, D. H. Lu, D. L. Feng, L. L. Miller, H. Takagi, and Z.-X. Shen, *Phys. Rev. B* **67**, 165101 (2003).
- ⁴⁵N. Harima, A. Fujimori, T. Sugaya, and I. Terasaki, *Phys. Rev. B* **67**, 172501 (2003); H. Yagi, T. Yoshida, A. Fujimori, Y. Kohsaka, M. Misawa, T. Sasagawa, H. Takagi, M. Azuma, and M. Takano, *ibid.* **73**, 172503 (2006).
- ⁴⁶T. D. Stanescu and G. Kotliar, *Phys. Rev. B* **74**, 125110 (2006).
- ⁴⁷See Fig. 4(a) in T. Yoshida, X. J. Zhou, D. H. Lu, S. Komiya, Y. Ando, H. Eisaki, T. Kakeshita, S. Uchida, Z. Hussain, Z.-X. Shen, and A. Fujimori, *J. Phys.: Condens. Matter* **19**, 125209 (2007).

- ⁴⁸N. P. Armitage, F. Ronning, D. H. Lu, C. Kim, A. Damascelli, K. M. Shen, D. L. Feng, H. Eisaki, Z.-X. Shen, P. K. Mang, N. Kaneko, M. Greven, Y. Onose, Y. Taguchi, and Y. Tokura, *Phys. Rev. Lett.* **88**, 257001 (2002).
- ⁴⁹A. Macridin, M. Jarrell, T. Maier, P. R. C. Kent, and E. D’Azevedo, *Phys. Rev. Lett.* **97**, 036401 (2006).
- ⁵⁰G. Dopf, J. Wagner, P. Dieterich, A. Muramatsu, and W. Hanke, *Phys. Rev. Lett.* **68**, 2082 (1992).
- ⁵¹P. Unger and P. Fulde, *Phys. Rev. B* **48**, 16607 (1993).
- ⁵²P. Wrobel, W. Suleja, and R. Eder, arXiv:0805.4129 (unpublished).
- ⁵³B. P. Stojković and D. Pines, *Phys. Rev. B* **55**, 8576 (1997).
- ⁵⁴H. Yamase and W. Metzner, *Phys. Rev. B* **75**, 155117 (2007).
- ⁵⁵S. Chakravarty and H.-Y. Kee, *Proc. Natl. Acad. Sci. U.S.A.* **105**, 8835 (2008).
- ⁵⁶K. Park and S. Sachdev, *Phys. Rev. B* **64**, 184510 (2001).
- ⁵⁷M. Sutherland, S. Y. Li, D. G. Hawthorn, R. W. Hill, F. Ronning, M. A. Tanatar, J. Paglione, H. Zhang, L. Taillefer, J. DeBenedictis, R. Liang, D. A. Bonn, and W. N. Hardy, *Phys. Rev. Lett.* **94**, 147004 (2005).
- ⁵⁸G. Baskaran, arXiv:0709.0902 (unpublished).